Advances and challenges in commercializing radiative cooling

J. Liu [a], Z. Zhou [a, *], J. Zhang [a], W. Feng [b, **], J. Zuo [c]

[a] *Tianjin Key Laboratory of Indoor Air Environmental Quality Control, Key Laboratory of Efficient Utilization of Low and Medium Grade Energy, School of Environmental Science and Engineering, Tianjin University, Tianjin, China*
[b] *Lawrence Berkeley National Laboratory, Berkeley, CA, USA*
[c] *School of Architecture & Built Environment, The University of Adelaide, Adelaide, 5005, Australia*

ARTICLE INFO

ABSTRACT

Radiative cooling (RC) dissipates terrestrial heat to outer space through the atmospheric window, without external energy input and production of environmental pollutants. More and more efforts have been devoted to this clean promising cooling technology; thus diverse radiative coolers have emerged. However, the performance, cost, and effectiveness of various radiative coolers are not exactly the same. In addition, the large-scale application of RC technology is impeded by the low energy density, uncontrollable cooling power, and limited sky-facing area. Here, we critically review the recent progress of RC technology, evaluate the cooling performance of various radiative coolers, and discuss the challenges and feasible solutions to commercialize RC technology. Furthermore, valuable insights are provided to make new breakthroughs in this field.

© 2019 Elsevier Ltd. All rights reserved.

1. Introduction

Radiative cooling (RC) can eliminate heat to outer space at 3K through the atmospheric window, not only reducing the fossil energy consumption through refrigeration but also mitigating the global warming effect. As a promising next-generation cooling technology, RC has been extensively investigated in the past decades [1–5]. However, daytime RC has not been demonstrated until recently [6]. Different from nocturnal RC, solar absorption is the critical factor for daytime RC, instead of mid-infrared emission. Therefore, it is imperative to simultaneously achieve high mid-infrared emission and low solar absorption to break through the day and night restriction and achieve all-day RC.

With the development of nanophotonics, there emerge more and more opportunities to design the radiative coolers for different applications. To achieve daytime RC, it is essential to minimize the solar absorption and maximize mid-infrared emission. Specifically, radiative coolers can achieve high solar reflectivity via exploiting high reflective metal or porous structure. For mid-infrared emission, when the photonic structure feature size is close to the wavelength, through the interference effect, one can tailor different spectral resonances to design the desired photonic radiative coolers, including planar multilayer one dimensional (1D) structure, multilayer two dimensional (2D) structure, metamaterial and metasurface.

Although scalable radiative coolers enable this technology to manufacture on a large scale [7,8], the high cost still hinders the progress significantly. Here, we review state-of-the-art advances in RC and highlight the efforts to improve the infrared emission and reduce the solar absorption of radiative coolers. We then discuss the promising applications, including building cooling (BC), photovoltaic cooling (PC), cryogenic cooling (CC), and energy harvesting (EH), each of which requires different spectral emission profiles. Subsequently, we presented an overview of main challenges to commercialize this promising technology, including the low energy density, uncontrollable cooling power, and limited sky-facing area. In addition, we provided the valuable insights to facilitate the large-scale application and make new breakthroughs in the RC field.

2. Principles of RC

We start with a discussion of net cooling power in this review. From the thermodynamic point of view, the cooling performance of radiative coolers under direct sunlight is explored. Considering a radiative cooler with the spectral and angular emissivity $\varepsilon(\lambda, \theta)$ at a temperature of T_r, exposed to the direct sunlight, the net RC power can be expressed as follows:

---

* Corresponding author.
** Corresponding author.
E-mail addresses: zhuazhou@tju.edu.cn (Z. Zhou), weifeng@lbl.gov (W. Feng).

$$P_{cool}(T_r) = P_r(T_r) - P_a(T_a) - P_{sun} - P_{cond+conv} \qquad (1)$$

The radiation intensity of the radiative cooler with area A is defined as follows:

$$P_r(T_r) = 2\pi A \int_0^{\frac{\pi}{2}} d\theta \sin\theta \cos\theta \int_0^\infty d\lambda I_B(T_r, \lambda)\varepsilon(\lambda, \theta) \qquad (2)$$

And the atmospheric radiation intensity absorbed by the radiative cooler is defined as follows:

$$P_a(T_a) = 2\pi A \int_0^{\frac{\pi}{2}} d\theta \sin\theta \cos\theta \int_0^\infty d\lambda I_B(T_a, \lambda)\varepsilon(\lambda, \theta)\varepsilon_{atm}(\lambda, \theta) \qquad (3)$$

where $I_B(T, \lambda)$ is the spectral radiation of a black body at the temperature of T_r or T_a (ambient temperature) at any wavelength λ by Plank's law.

The spectral and angular emissivity of the atmosphere is given as follows:

$$\varepsilon_{atm}(\lambda, \theta) = 1 - t(\lambda)^{1/cos(\theta)} \qquad (4)$$

where, $t(\lambda)$ is the atmospheric infrared transmittance in the zenith direction and can be available from MODTRAN (2018).

To explore the RC performance in different regions under different atmospheric environment, some atmospheric emission models are used in some studies. The model used most is proposed by Berdahl et al. [4].

$$\varepsilon_a = 0.711 + 0.56\left(\frac{T_{dp}}{100}\right) + 0.73\left(\frac{T_{dp}}{100}\right)^2 \qquad (5)$$

where, T_{dp} is the dew point temperature. Li et al. [9] corrected the model with the atmospheric emissivity in different regions of the United States, and the relative error of the model is less than 5%. Thus, the model can accurately depict the atmospheric infrared emissivity in different regions.

For cloudy days, the aforementioned model needs to be modified according to the cloud amount in the sky using Equation (6) [10].

$$\varepsilon_{atm} = (1 + 0.026C)\varepsilon_a \qquad (6)$$

where, C is the amount of clouds, which can be estimated by the area of clouds in the sky, from 0 to 10, indicating cloudless to cloudy days.

The solar radiation absorbed by the radiative cooler must be considered for daytime RC. And the solar intensity absorbed by the radiative cooler is expressed as follows:

$$P_{sun} = A \int_0^\infty d\lambda \varepsilon_s(\lambda, 0)I_{solar}(\lambda) \qquad (7)$$

where, $\varepsilon_s(\lambda, 0)$ is the solar absorptivity of the radiative cooler at a fixed angle 0. For the opaque radiative coolers, the solar absorptivity is given by $\varepsilon_s(\lambda, 0) = 1 - r_s(\lambda, 0)$, where $r_s(\lambda, 0)$ is the solar reflectivity, which can be measured by UV-Vis-NIR spectrophotometer equipped with integrating sphere.

Non-radiative heat exchange (NRHE) includes convection and conduction between the radiative cooler and the surrounding. For above-ambient cooling, for example, photovoltaic cooling, NRHE is conducive to heat dissipation, whereas for subambient cooling,

NRHE is adverse to the reduction of radiative cooler temperature. And the wind cover with high mid-infrared transmittance is used to reduce the NRHE. The NRHE intensity can be expressed as follows:

$$P_{cond+conv}(T_r, T_a) = Ah_c(T_a - T_r) \qquad (8)$$

where, h_c is the combined NRHE coefficient stemming from the conductive and convective heat exchange. Early experimental studies on solar flat panel reveal that the effect of wind speed on NRHE can be quantified by linear correlation [11,12].

$$h_c = a + bv \qquad (9)$$

3. Advances in RC

3.1. Suppression of solar absorption

The key to achieve daytime RC is to suppress the solar absorption of the radiative coolers. Decades ago, a high-infrared transparent polymer embedded with nanoparticles (e.g. ZnS, ZnO, or TiO$_2$) was used as a solar reflector, that is, spatially above the radiative coolers. Nevertheless, the radiative coolers cannot be cooled below ambient because of its incapability to effectively reflect sunlight (less than 85%) (Fig. 1a) [13,14]. However, with the high reflective metal coating (e.g. Ag, Al), the solar reflectivity of radiative coolers can be improved to achieve daytime RC. However, it is worth noting that the solar transmissivity of emission layers must be high enough to reduce the solar absorption (Fig. 1b) [15,16]. Similarly, it is viable to reduce the solar absorption by integrating the emitters with alternating high-index and low-index multilayer structure, which can further improve the solar reflectivity (Fig. 1c) [6,17,18].

It is well established that Mie scattering can be used to reduce the solar absorption of radiative coolers, with benefits of avoiding the use of precious metals and reducing the overall cost of RC technology. By optimizing the TiO$_2$ coating [19,20], the SiO$_2$ coating [21], the porous polymer [8], cooling wood [22], and aluminum phosphate [23], the scattering mean free path can be minimized, thus the solar absorption can be effectively reduced. Meanwhile, the impedance matching between the radiative coolers and the surrounding medium (air) is effectively improved, leading to a slight increase of the mid-infrared emission (Fig. 1f). In addition, one can also take advantage of the angular confinement of the solar flux and use sunshade to prevent radiative coolers from absorbing the direct sunlight, and the absorption of diffuse sunlight can be suppressed by nanoporous polyethylene film [24,25]. Thus, radiative coolers can achieve less than 5% solar absorptivity (Fig. 1d and e). Moreover, with the development of nanophotonics, near-unity of solar reflectivity can be achieved with the infrared transparent solar spectral grating (Fig. 1g) [26] and all-dielectric metasurfaces, consisting of nanoscale high-index resonators [27,28]. Furthermore, another method to suppress the solar absorption is to use solar absorption materials (e.g. photothermal, photoelectric, or filter layer) to harness solar energy, not only reducing the corresponding solar absorption but also making effective use of solar energy (Fig. 1h). However, it is worth noting that the solar absorption materials must have a high-infrared transmissivity to implement RC.

3.2. Improvement of mid-infrared emission

There are enormous approaches to improve mid-infrared emission of radiative coolers. This review only covers the recent proposed photonic radiative coolers. With the development of
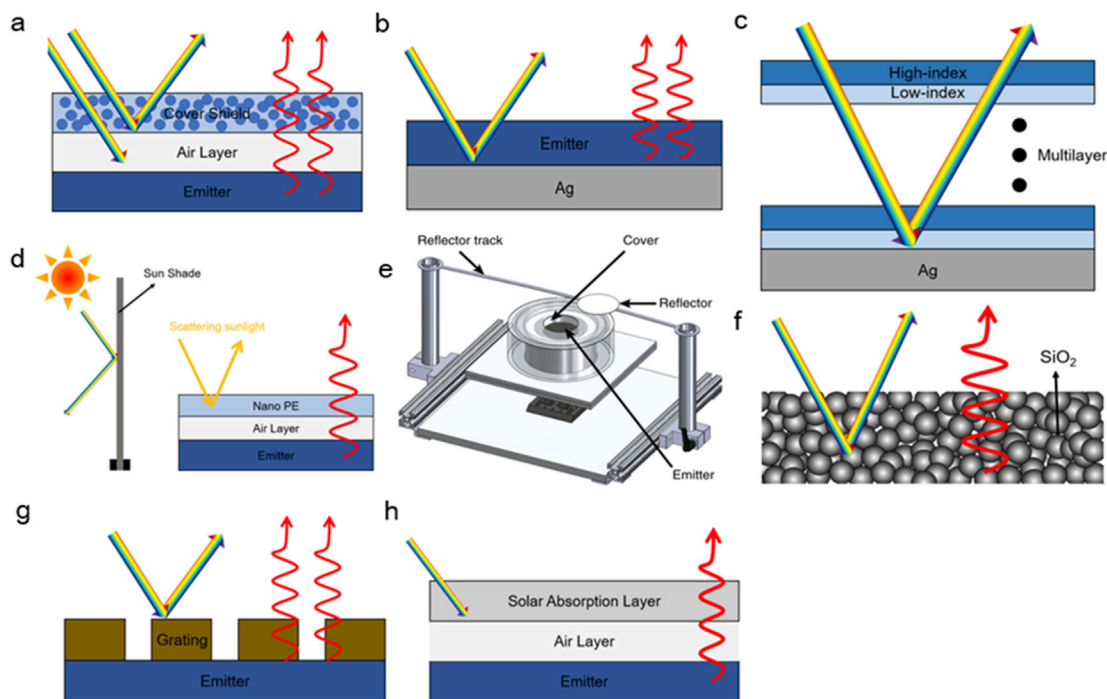
Fig. 1. Suppression of solar absorption. (a) A wind cover consisting of the high-infrared transmission polymer (e.g. polyethylene) and nanoparticles (ZnS, ZnO, or TiO_2) is spatially above the radiative cooler. (b) High reflective metal layers (e.g. Ag, Al) are coated under the emitters, which have high solar transmissivity. (c) Alternating high-index and low-index multilayer structure is integrated with the emitter to suppress the solar absorption. (d) High reflective shade is used to prevent emitter from absorbing direct solar radiation and nanoporous polyethylene film is used to suppress the absorption of diffuse sunlight. (e) Experimental device of the directional daytime RC with a polished aluminum reflector to reflect the direct sunlight [25]. Reproduced with permission from Bhatia et al., Nat. Commun. 9 (2018) 5001. Copyright 2018 Nature Publishing Group. (f) The SiO_2 coating can effectively reduce the solar absorption and increase the mid-infrared emission. (g) An infrared transparent solar spectral grating can suppress the solar absorption. (h) The materials absorbing solar radiation (photothermal, photoelectric, or filter layer) can reduce the solar absorption of the emitters. RC = radiative cooling.

nanophotonics, the spectral profiles of radiative coolers can be tailored according to actual applications.

3.2.1. One dimensional and 2D photonic structure

When the feature size of photonic structure is close to the wavelength, the interference effect can tailor different spectral resonances to design the desired photonic radiative coolers. Planar multilayer 1D structure [6,24,29], multilayer 2D structure [18,30], metamaterial [31], and metasurface [32] can all achieve low sunlight absorption and high mid-infrared emission. By optimizing the planar 1D structure of materials (e.g. SiO_2, TiO_2, Al_2O_3, and HfO_2), which is loss in the mid-infrared wavelength range and not lossless in the solar wavelength range, one can achieve less than 5% solar absorption and high mid-infrared emission (Fig. 2a).

For instance, owing to phonon polariton resonance, SiO_2 has a very high absorption peak near 9.3 μm. By tailoring the emission profile of HfO_2 and SiO_2 in infrared wavelength range and coating with the reflective layer, consisting of the alternating HfO_2 (high-index) and SiO_2 (low-index) layer and silver coating, daytime RC is achieved for the first time, but the radiative cooler has an infrared emissivity of less than 0.7 in the atmospheric window [6]. In addition, the proposed photonic structure achieved the selective emission in the atmospheric window (8−13 μm), mainly due to the special phonon polariton resonance of the materials in the atmospheric window and the special number and thickness of layers. Conversely, some researchers optimize the photonic structure proposed by Raman et al. [6] to achieve higher emissivity in the atmospheric window. And Al_2O_3 [16] or TiO_2 [29] was used to replace the HfO_2 layer, indeed with the reasonable optimization, they achieved the emissivity of 0.8 and 0.96 in the atmospheric window with the similar structure, respectively. However, the

photonic structure loses the characteristic of selective emission. The main reason behind is that Al_2O_3 and TiO_2 have the strong phonon resonance absorption (as revealed by the imaginary part of permittivity) beyond the atmospheric window (e.g. in the wavelength range of 20−25 μm). Even with the reasonable design and optimization, for example, needle optimization, simulated annealing, and jump method, one must make a trade in spectral selectivity and high emissivity owing to the lack of suitable materials and overall cost. To date, most researchers incline to use the radiative coolers with high emissivity, owing to the low available energy density of the RC technology.

Compared with the planar multilayer 1D structures, multilayer 2D structures have a higher degree of freedom, which is beneficial to tailor the spectral emission (Fig. 2b). By introducing 2D periodic array of square air holes in SiO_2 and SiC layers, as well as multilayer TiO_2 (high-index) and MgF_2 (low-index) 1D structure with silver coating as the bottom, the 2D radiative cooler achieves a solar absorption of 97% and near-unity mid-infrared emission in the atmospheric window and the second atmospheric window (16−25 μm) [13]. By analogy with moth-eye effect, near-unity mid-infrared emission can be achieved in the wavelength range of 8−27 μm using multilayer Al_2O_3 and SiO_2 micropyramid arrays [30]. It is worth noting that the two 2D structures can exploit a high emissivity in the second atmospheric window, helping to improve the overall cooling power.

3.2.2. Metamaterial and metasurface

In addition, metamaterials have the advantage of supporting both local and lattice resonance modes, which also increase the flexibility of design. Owing to the slow light modes, the special 2D metamaterial structure, consisting of a symmetrical conical
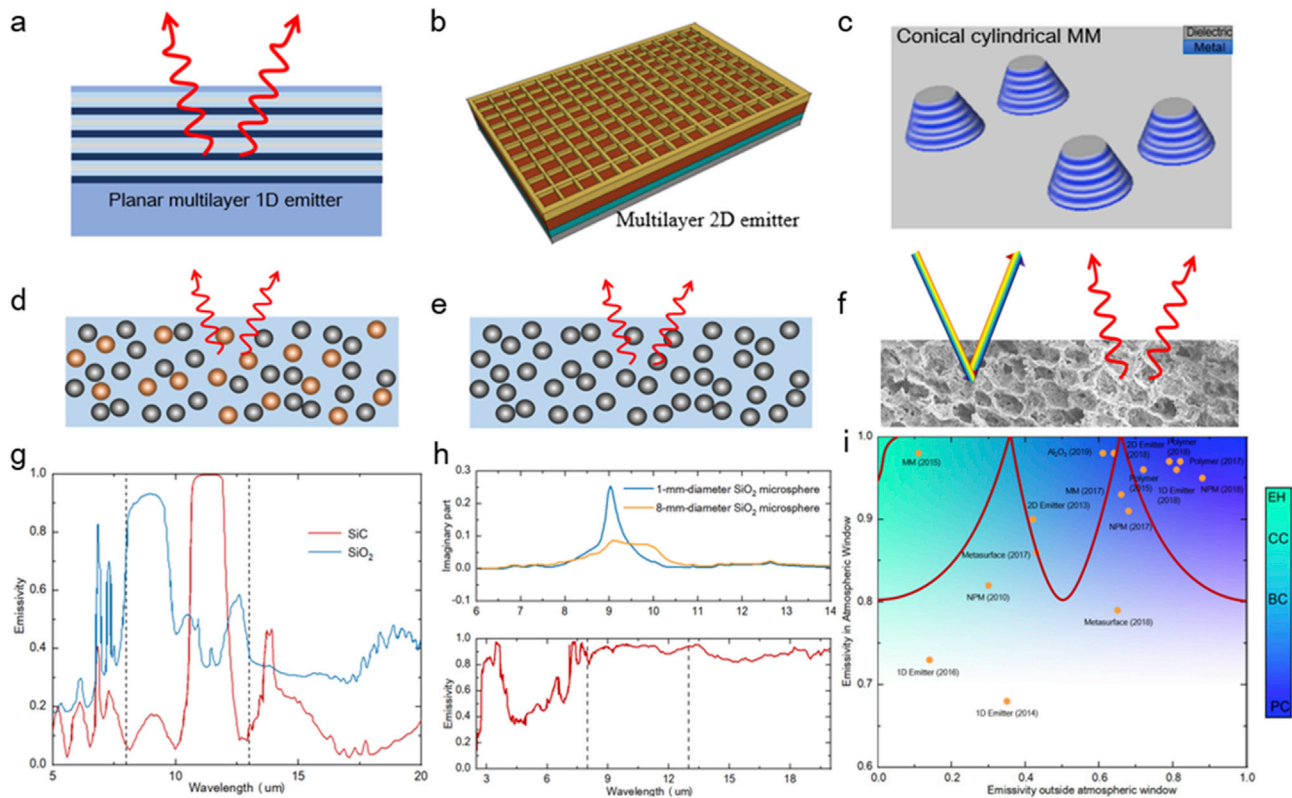
Fig. 2. Improvement of mid-infrared emission. (a, b) Schematics of a planar multilayer 1D structure and multilayer 2D structure, consisting of different index dielectric. (c) Image of conical cylindrical metamaterial, comprising of alternate metal and dielectric. (d, e) Schematics of NPMs, including two complementary nanoparticles and a single nanoparticle, respectively. (f) Image of hierarchically porous polymer coating [33]. Adapted with permission from Mandal et al., Science 362 (2018) 315−319. Copyright 2018 the American Association for the Advancement of Science. (g) The infrared spectral complementarity of SiO_2 and SiC in the atmospheric window. Reproduced with permission from Gentle et al. Nano Lett. 10 (2010) 373−379. Copyright 2010 American Chemical Society. (h) The imaginary part of refractive index for the glass-polymer hybrid metamaterial (top) and the corresponding infrared emissivity (below) [7]. Reproduced with permission from Zhai et al., Science 355 (2017) 1062−1066. Copyright 2017 the American Association for the Advancement of Science. (i) Classification of the recently proposed radiative coolers according to the infrared emissivity inside and outside the atmospheric window, which are applicable to different directions. From left to right, EH, CC, BC and PC are represented with different shades of color. Reference list: NPM (2010) [33], 2D emitter (2013) [18], 1D emitter (2014) [6], metamaterial (MM) (2015) [31], polymer (2015) [17], 1D emitter (2016) [24], metasurface (2017) [32], MM (2017) [7], NPM (2017) [20], polymer (2017) [35], 2D emitter (2018) [30], polymer (2018) [8], NPM (2018) [21], metasurface (2018) [103], 1D emitter (2018) [29], Al_2O_3 (2019) [36]. EH = energy harvesting, CC = cryogenic cooling, BC = building cooling, PC = photovoltaic cooling, NPM = nanoparticle mixture material.

cylindrical arrays of multilayer metal aluminum and dielectric germanium, achieves near-unity infrared emissions in the wavelength range of 8−13 μm (Fig. 2c) [32]. Owing to the introduction of metal with the low solar transmissivity, the daytime RC cannot be achieved with the silver coating. However, the 2D metamaterial structure can achieve daytime RC with a high reflective sunshade or an infrared transparent solar spectral grating in Fig. 1g and h. Moreover, the dielectric resonance metasurface can support many resonance modes and tailor the spectral profiles of radiative coolers efficiently. The phosphorous-doped n-type silicon is combined with the Ag coating (reflecting non-resonant band) to form a metasurface to realize broadband plasma resonance, thereby achieving high-infrared emission in the wavelength range of 4−13 μm [32].

Although photonic structures can effectively tailor the emission of radiative coolers, multilayer 2D structures, metamaterials, and metasurfaces all use complex manufacture procedures (e.g. electron beam lithography, nanoimprint lithography, and reactive ion etching). Thus, the immaturity and high cost of micro-nanofabrication technology have limited their potential applications on a large scale. For planar multilayer 1D structure, the process of gel precipitation and magnetron sputtering can be used, but the high cost of the processing technology and materials still impede the large-scale application of the structure.

3.2.3. Scalable RC materials

In recent years, more and more efforts have been devoted to the scalable RC materials. Nanoparticle mixture materials [7,33] and polymer materials [8,17,34,35] are the first choice for large-area applications, because of low cost and mature manufacture technology. It is well established that SiO_2 nanoparticles stand out with a surface phonon resonance (electric dipolar) for the wavelength range of 8−10 μm, which cannot cover the whole atmospheric window. For the wavelength range of 10−13 μm, some other nanoparticles can be used to achieve the higher emissivity in the whole atmospheric window, for example, SiC [33] and $CaMoO_4$ [36] (Fig. 2d and g).

In addition, taking advantage of phonon-enhanced high-order resonances (both electric and magnetic modes), the polar dielectric SiO_2 nanoparticles (particle size of 8 μm) are randomly embedded in the polymer polymethyl-pentene (TPX) to enhance the infrared emission. The imaginary part of refractive index for the dielectric SiO_2 nanoparticles with different particle sizes was plotted in Fig. 2h, and it can be clearly seen that the nanoparticles with the particle size of 8 μm have the resonance absorption peak covering the atmospheric window. However, owing to the infrared absorption of the polymer (TPX) beyond the atmospheric window, the metamaterial film lost the spectral selectivity in the atmospheric window (Fig. 2e). Perhaps, low density polyethylene can be the

suitable substrate for the metamaterial to achieve the better spectral selectivity because of low absorption of the thin polyethylene film in the mid-infrared band. But the poor weather resistance of the polyethylene film may place some restrictions on the application of metamaterial film. In addition, it is worth noting that the metamaterial can be fabricated roll to roll with advantages of low cost and scalable fabrication [7]. Similarly, one can further tune the particle size of SiO_2 microspheres (e.g. 2 μm), optimize the filling rate and scattering mean free path, and choose spraying or colloidal precipitation to fabricate the radiative coolers, not only effectively scattering solar radiation but also enhancing the mid-infrared emission [21].

Moreover, similar to nanoparticles embedded in polymer, one can use the materials with the high-infrared emission to form the porous structure to achieve the low solar absorption and high mid-infrared emission. In this way, near-unity emission in the wavelength range of 7−18 μm can be achieved by porous polymer coating with the hierarchical pore near 0.2 μm and 5 μm to effectively scatter the visible and near-infrared light, respectively. Meanwhile, the hierarchically porous polymer has the higher mid-infrared emissivity than the bulk polymer because of the better impedance matching of the porous polymer and the air (Fig. 2f) [8]. It is worth noting that the phase inversion method used in the porous polymer is simple, inexpensive, and scalable to reduce the overall cost of RC technology. However, owing to the vibration absorption of the polymer beyond the atmospheric window, the hierarchically porous polymer loses the spectral selectivity, and it is still a challenge to seek out suitable materials to achieve the spectral selective radiative coolers, using the phase inversion method. Similarly, the effective medium theory is used to optimize the porosity of Al_2O_3, produced by chemical anodization. As a result, the impedance matching between the radiative cooler and surrounding medium (air) is improved, and the emissivity of Al_2O_3 in mid-infrared wavelength range is improved significantly without affecting the solar transmissivity [37].

3.2.4. Classification of RC materials

The solar absorptivity can be used to evaluate the performance of various approaches to suppress the solar absorption. In general, less than 10% solar absorptivity can meet the need of daytime RC in the arid mid latitudes. However, it is more complex to evaluate the infrared emission performance of radiative coolers. Generally, the net cooling power at ambient temperature and stagnation temperature has been the common indicators to evaluate the infrared emission performance. However, the standard of ambient temperature and the cooling power used in previous studies varied significantly (e.g. some use the maximum value [35], whereas others adopt the average value [8,13]). Moreover, the NRHE has a significant impact on stagnation temperature. For instance, the average stagnation temperature of 37 K below ambient can be achieved in vacuum [24], whereas the radiative cooler temperature below ambient cannot be achieved without cover shield [20]. It is difficult to compare the infrared emission performance of different radiative coolers with these two indicators. However, it is recognized that the above two indicators are the concretion of the radiative coolers' infrared emission profiles. Thus, the performance of different radiative coolers can be evaluated by comparing the average infrared emissivity inside and outside the atmospheric window. To that end, we summarized the infrared emission profiles of radiative coolers in recent years and classified the radiative coolers into four main applications, that is, BC, PC, CC, and EH (Fig. 2i).

3.3. Promising RC applications

There are extensive applications of RC including BC, PC, CC, and EH. Especially for remote areas, RC can be used to refrigerate, even to cool below the dew point temperature, and harvest fresh water [38].

3.3.1. Building cooling

BC is similar to the aforementioned cooling devices. In general, wind cover is required to suppress the non-radiation heat exchange. To date, polyethylene with about the thickness of 10 μm is mainly used for subambient RC. However, due to low strength, thin polyethylene does not support the cooling devices making into a vacuum chamber or filled with rare gases to further reduce the heat coefficient. In addition, with the effect of ultraviolet radiation, the thin polyethylene ages in a fast speed. Despite the high strength, the utilization of ZnS and ZnSe sheets in BC is limited because of their low solar transmissivity and high cost.

Furthermore, unlike the subambient cooling devices, it is essential to have a large cooling power for the radiative coolers, due to the large thermal mass of buildings. Thus, aside from enabling a high emissivity in the atmospheric window, it is also essential to have a certain emissivity in other infrared wavelength range, which is crucial to improve the cooling power and quickly cool down the large thermal mass. Owing to the large thermal resistance of the building roof, the high reflective cooling material directly laid on the roof can only partially reduce the cooling load of the buildings and cooperate with air conditioning system (e.g. cool roof). It is not an effective approach to cool buildings below the ambient. For low-energy buildings (e.g. passive buildings), the peak heat load [39] in summer is less than $30/W/m^2$, which is lower than the daytime RC power under clear and cloudless sky ($100/W/m^2$). In other words, with appropriate roof heat exchange, the cooling demand in summer can be met with less than 1/3 of the roof area or even no longer relying on the air conditioning system.

However, for multistorey buildings, RC cannot meet the whole cooling demand of buildings because of limited roof area. To date, the application of RC in buildings mainly uses the indirect way, cooling the working fluids and coupling with the air conditioning system through the plate heat exchanger (Fig. 3a). Theoretically, 21% of the electricity can be saved during the entire summer season [40]. Similarly, the integration of radiative coolers with multichannel instead of metal coil can preprocess the working fluids of air conditioning system and achieve the maximum energy efficiency by coupling with the cold storage system (Fig. 3b) [41]. The flow rate of working fluid in those two systems is relatively slow (0.29 L/min/m² and 0.44 L/min/m², respectively) because of the low energy density of RC. As a result, it is not easy to couple with the air conditioning system in actual operation and have significant cooling performance at the same time. However, this RC system can flexibly control the cooling input to the building and is suitable for areas where the temperature varies greatly during the day and night. Therefore, the indirect way, coupling with air conditioning system has a better prospect for existing multistorey buildings. On the contrary, for new buildings or factories with large roof area, especially in remote areas, it is more appropriate to adopt direct cooling method, that is, coupling with buildings.

3.3.2. Photovoltaic cooling

PC includes solar cell cooling, concentrated photovoltaic system cooling, and thermal photovoltaic system cooling. Crystalline silicon solar cells are the most widely used solar cells, which have intrinsic limitation on the theoretical conversion efficiency (33.7% based on Shockley and Queisser's analysis) [42], and the actual conversion efficiency of crystalline silicon solar cells is as low as 20%. Previous studies have shown that every 1 °C temperature rise results in a relative efficiency decline of about 0.45% for crystalline silicon solar cells [43], and the aging rate of solar cells doubles for every 10 °C increase. Therefore, the conversion efficiency and
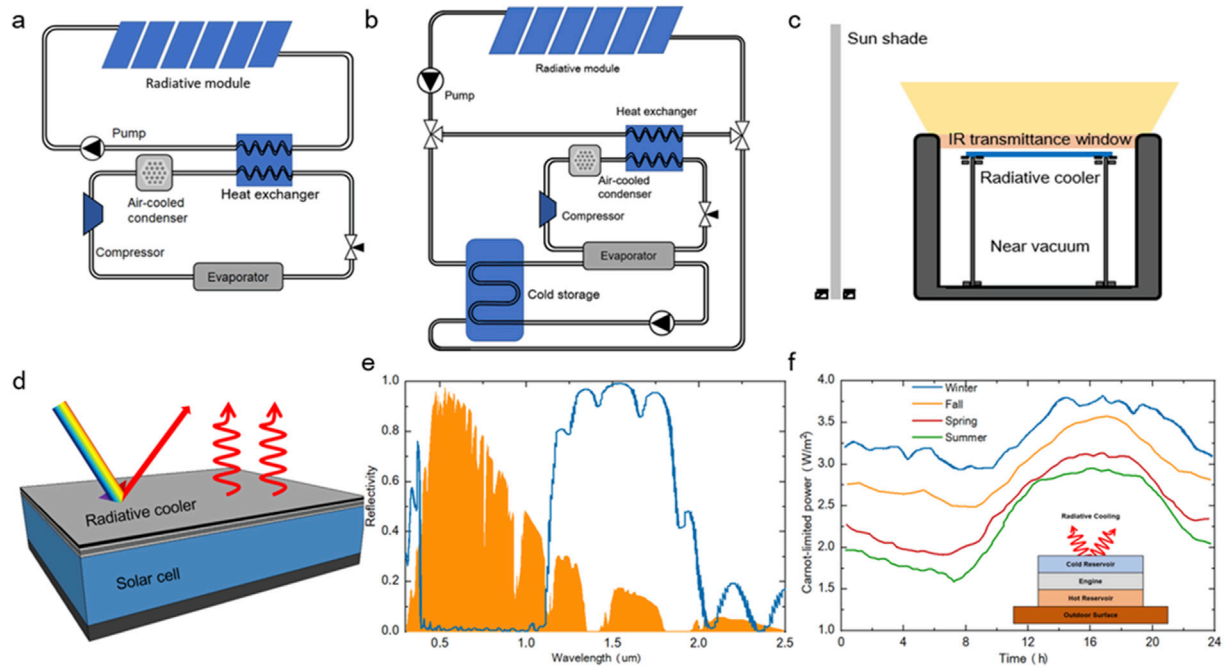
Fig. 3. Main application of radiative cooling. (a) Schematic of the combination of radiative cooling module and air conditioning system through the heat exchange. (b) Schematic of the composite system with radiative cooling module, air conditioning system, and cold storage system. (c) Schematic of the cryogenic cooling setup including sunshade, radiative cooler, infrared transmittance window etc., (d) Schematic of photovoltaic cooling with a selective emitter to reflect the ineffective solar radiation (above 1.1 μm). (e) Reflective spectrum of the selective photonic cooler and the AM 1.5 solar spectrum (orange) is provided for reference [48]. Fig. 3d and e are reproduced with permission from Li et al., ACS Photonics 4 (2017) 774–782. Copyright 2017 American Chemical Society. (f) The instantaneous Carnot-limited power for each of the four seasons. The inset image depicts the schematic of EH [52]. Reproduced with permission from Byrnes et al., Proc. Natl. Acad. Sci. 111 (2014) 3927–3932. Copyright 2014 National Academy of Sciences. EH = energy harvesting.

service life of solar cells can be improved by reducing the actual operating temperature of solar cells.

Different from BC, the operating temperature of solar cells is above the ambient, and there exists no need for a highly transparent wind cover. Meanwhile, due to the high operating temperature, NRHE is beneficial to the heat dissipation for solar cells. If emitters are directly combined with bare photovoltaic panels, the improvement of the actual the conversion efficiency is limited [44,45] and even the service life of solar cells may be reduced due to the poor packaging. Previous studies have revealed that the quartz used for encapsulating solar cells has high-infrared emissivity, thus it is seemingly not essential to use RC to reduce the solar cell temperature [46]. However, quartz has a large absorption dip near the wavelength of 9 μm, thus the emissivity in the atmospheric window is only about 85%. By coating the polydimethylsiloxane (PDMS) film, the quartz has an ideal emissivity in the atmospheric window without affecting the solar transmissivity, therefore, the temperature of solar cells can be further reduced [47].

Further research studies reveal that the actual effective spectral range of crystalline silicon solar cells is within 0.3−1.1 μm, and the rest solar energy is converted into heat, further reducing the overall solar cell conversion efficiency. If the ineffective solar absorption can be effectively suppressed, the operating temperature of solar cells will be enormously reduced (Fig. 3d). The absolute conversion efficiency can be improved by about 1% by introducing 1D [48] and 2D [49] photonic structures to make into the selective emitters with high solar reflectivity more than the wavelength of 1.1 μm and high mid-infrared emission (Fig. 3e). For concentrated photovoltaic system and thermal photovoltaic systems, the cooling effect of the photonic emitter is more significant [50,51]. Owing to the cost and immature processing technology of photonic structures, it is, to date, difficult to commercialize the photonic structures, selectively

reflecting solar radiation. However, inspired by hierarchically porous polymer coating [8], the efficient cooling of solar cells can be achieved by tailoring the pore size distribution of radiative materials to scatter the solar radiation more than the wavelength of 1.1 μm.

3.3.3. CC and EH

CC can be used in many fields, for example, in freezers and biomedical devices. By combining with a hard, high-transparent wind cover to reduce NRHE (in vacuum), the selective radiative cooler can achieve a temperature drop of up to 42 °C, and theoretically the maximum temperature drop can reach 60 °C (Fig. 3c) [24]. However, the selective radiative cooler has fairly low cooling power and needs long time to achieve the large temperature drop. The reason behind is that as the radiative cooler temperature declines, the net cooling power is increasingly lower.

In addition, one can use the radiative cooler as a cold reservoir and the ambient as a hot reservoir, thus, renewable energy can be achieved from this heat flow, namely EH. When coupled with Carnot cycle, the maximum output power is $P_{Cool}(T_{Hot}/T_{Cold}-1)$, where T_{Hot}, T_{Cold}, and P_{Cool} are hot reservoir temperature, cold reservoir temperature, and net RC power, respectively. For the real radiative coolers, net RC power decreases with the decrease of radiative cooler temperature. Therefore, it is imperative to consider both cooling power and T_{Cold} to choose the suitable radiative coolers. Even after optimization, the maximum average output power is still about 2.7/W/m^2, when the ambient is used as the hot reservoir. Nevertheless, when the hot reservoir with high temperature (e.g. solar absorbing material) was used, the maximum output power may be five times higher (Fig. 3f) [52]. Further using the hot reservoir with higher temperature (e.g. industrial waste heat), the power output can be more significant. Moreover, relative

to solar energy affected by time and other factors, RC is always running. It is worth noting that the Earth continuously emits about 10^{17} W thermal radiation, which is theoretically enough to meet human beings' energy needs. Therefore, harvesting the emissive energy is highly promising with the development of RC technology. Similarly, semiconductors can be used to implement EH, such as rectifier antennas [53,54]. But the auger recombination may impede the practical application of EH [55]. Nevertheless, the massive energy potential of EH warrants further investigation.

4. Challenges and feasible solutions to commercialize RC technology

4.1. Cooling power improvement

Low energy density of RC technology requires large areas to meet the cooling load, but the excessive RC areas not only increase the cost of system but also affect the operation of other devices on the roof. Therefore, improving the net cooling power plays a crucial role in the application of RC technology, especially for CC and EH. Here, we investigate critical factors of the net cooling power and discuss feasible solutions to improve the net cooling power.

We consider the dominant heat exchange pathways for the radiative cooler, including the radiation intensity $P_r(T_r)$, the absorption atmospheric radiation $P_a(T_a)$, the absorption solar radiation P_{sun}, and the heat exchange intensity via NRHE $P_{cond+conv}$ [Equation (1)]. To date, researchers have improved the mid-infrared emissivity to more than 95% in the atmospheric window [29,37], and further improvement of the infrared emissivity has less impact on the net cooling power, due to low energy density of RC. Recently proposed thermal extraction [56,57] using near-field radiation to extract evanescent waves may be applied in the RC field. However, it is still a challenge to implement the near-field technology in RC owing to the immaturity and high cost. In addition, researchers have designed the near vacuum RC device to reduce the $P_{cond+conv}$ as far as possible [24].

Although the solar reflectivity has reached 97% [6,17], further improvement of the solar reflectivity is still urgent because of the high energy density of the sunlight (up to 1000 W/m^2), that is, there still exists great potential to improve the net cooling power (approximately 30 W/m^2). In addition, atmospheric radiation is another significant factor, affecting the net cooling power. However, extremely few efforts have been devoted to the reduction of atmospheric radiation absorption. Thus, it is highly promising to improve the net cooling power through reducing the atmospheric radiation absorption.

4.1.1. Further reduction of solar absorption

To achieve the daytime RC, it is essential for radiative coolers to have a solar reflectivity of more than 90% in arid middle latitudes. With the high reflective metal coating (e.g. Ag), radiative coolers can achieve a solar reflectivity high enough to achieve the cooling effect under the direct solar radiation. Nevertheless, with the abundant absorption of ultraviolet light in the solar wavelength range, it is still a challenge for silver coating alone to further improve the solar reflectivity of the radiative coolers.

As discussed in Section 3.1, radiative coolers using Mie scattering to reduce the solar absorption can also achieve the cooling effect under the direct solar radiation. However, it is essential for the radiative coolers to have a thickness of at least 300 μm to achieve the solar reflectivity of more than 95%, for example, hierarchically porous polymer [8] and SiO$_2$ coating [21]. To further improve the solar reflectivity up to 99% or higher, the radiative

coolers must have the thickness of more than 800 μm. It is well established that the thicker the radiative coolers, the higher the corresponding cost. Such a high cost will seriously hinder the practical application of RC technology.

To simultaneously achieve the near-unity solar reflectivity and low cost, one can combine the high reflective metal coating and the Mie scattering layers. Sintered polytetrafluoroethylene (PTFE) is generally used as the inner coating of integrating spheres because of the exceedingly high diffuse reflectance from ultraviolet to near-infrared. Yang et al. [34] propose that the combination of high diffuse PTFE film and high reflective silver coating can address the tough problems. With the reasonable optimization, the 240 μm PTFE film was placed on the 300 nm silver coating, and the structure achieved a solar reflectivity of 99.1%, a record solar reflectivity in the RC field (Fig. 4a). However, because of the rough surface of the PTFE film, it is infeasible to simultaneously coat the silver film on the PTFE surface and achieve enough reflectivity. Thus, it may be hard for the proposed structure to put into practical application because of the poor heat exchange between the silver coating and the PTFE film.

Generally, the radiative coolers using Mie scattering, all having the rough surface, that is, the silver film cannot be directly coated on it. Thus, the combination of the emitters using Mie scattering and high reflective films may lead to a failure in practical application. Nevertheless, as we all know, the RC devices generally use wind covers to reduce the NRHE. And the combination of porous wind covers and the silver films may be a feasible solution to address the aforementioned problem. In addition, nano polyethylene (PE) films have been used to reduce the absorption of the diffuse sunlight by the radiative coolers [25]. We suppose that with the smaller pores, nano PE films may be used to scatter the ultraviolet in the solar wavelength range. Therefore, we do the corresponding research and find that nano PE films with the pore of 30−50 nm can scatter 80% of the ultraviolet in the solar wavelength range and simultaneously have an average transmittance of more than 96.6% (87% for the ordinary PE film with the same thickness). With the combination of nano PE film and the silver film, the RC devices achieve a solar reflectivity of 99% [58]. More importantly, the proposed structure can be applied in practice.

4.1.2. Reduction of atmospheric radiation absorption

Radiative coolers are generally reciprocal structures, following Kirchhoff's law, that is, the angular spectral absorption and emission are equal. If the atmospheric radiation absorption is reduced or even suppressed, not only the net cooling power can be effectively improved but also the RC application scope will be extended to areas with high humidity [59]. Even the limitation of the atmospheric window can be broken through, which means that the whole mid-infrared wavelength range can be used as the transmission channel.

It is well established that real radiative coolers generally have a directional distribution that the surfaces have high emissivity below a zenith angle of 60°. And the real radiative coolers have also directional dependence that the atmospheric radiation absorptivity increases with the increase of zenith angle. Thus, the inverted cone structure with the high reflectivity can simultaneously block the atmospheric radiation from the large zenith angle and enable the high emissivity of the radiative coolers. With the inverted pyramid structure plotted in the left of Fig. 4b, Jacobs et al. [60] have improved the RC power by 20%. And Chen et al. [24] used the inverted mirror cone to block the high atmospheric radiation and achieved the record temperature drop of 42 °C in the daytime. For the ordinary daytime RC (DRC) devices, it is not feasible to form a
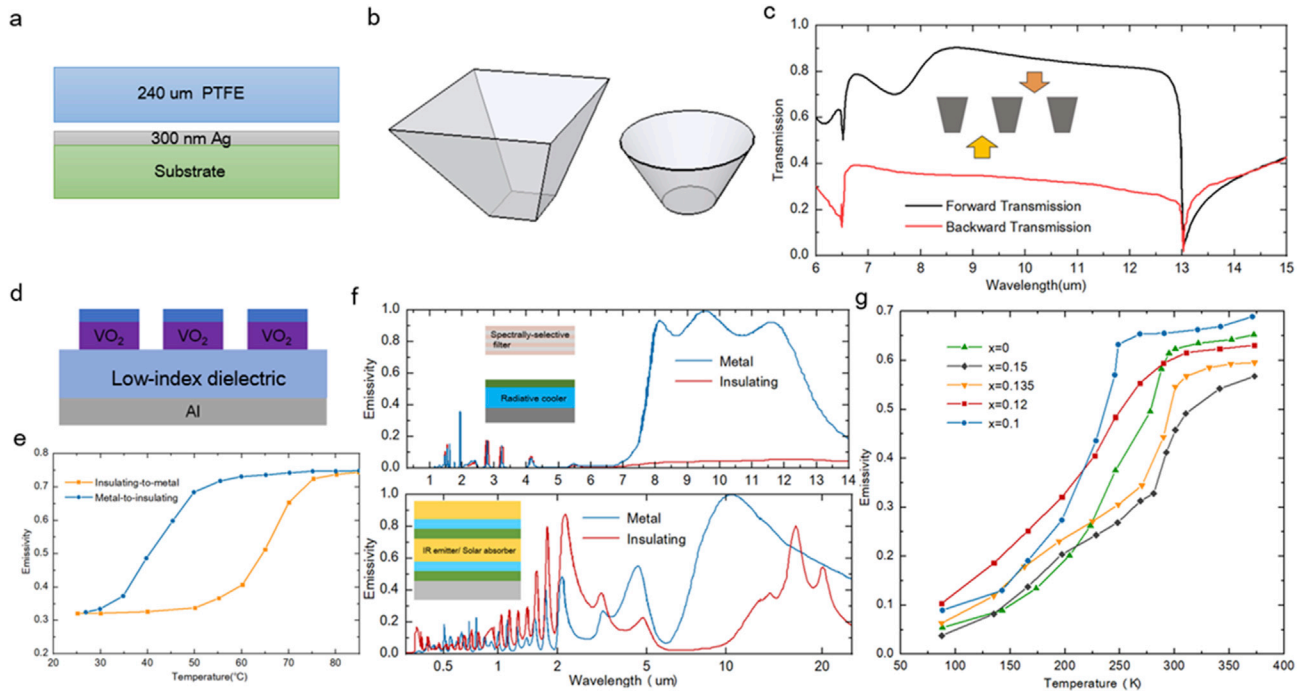
Fig. 4. Improvement and control of cooling power. (a) Schematic of the record solar reflexive structure high with the diffuse PTFE film and high reflective silver coating. (b) Schematics of inverted pyramid and cone for blocking the atmospheric radiation. (c) Forward and backward transmission with the infrared asymmetric transmission device in the 6−15 μm band [73]. The inset image is the schematic of non-reciprocal transmission. Reproduced with permission from Wong et al., Sol. Energy Mater. Sol. Cells 186 (2018) 330−339. Copyright 2018 Elsevier. (d) The image depicts schematic of the VO_2 controllable radiative cooler with high-reflection substrate and low-index dielectrics. (e) The change of emissivity with the temperature from insulating to metal and from metal to insulating [91]. Fig. 4d and e are reproduced with permission from Sun et al., ACS Photonics 5 (2018) 2280−2286. Copyright 2018 American Chemical Society. (f) The emissivity of the dynamic radiative cooler in the metal and insulating state of VO_2 and the inset image presents the schematic of the solar filter and the VO_2 radiative cooler (Top) [89]. Reproduced with permission from Ono et al., Opt. Express 26 (2018) A777−A787. Copyright 2018 the Optical Society. The bottom is the emissivity of VO_2 radiative thermostat in the metal and insulating state and the inset image depicts the schematic of the phase-change photonic structures for RC or solar absorption [90]. Reproduced with permission from Kort-kamp et al., ACS Photonics 5 (2018) 4554−4560. Copyright 2018 American Chemical Society. (g) Temperature dependence of infrared emissivity of $La_{0.7}Ca_{0.3-x}Sr_xMnO_3$ with different doping level (x) [92]. Reproduced with permission from Fan et al., Appl. Therm. Eng. 51 (2013) 255−261. Copyright 2013 Elsevier. PTFE = polytetrafluoroethylene.

vacuum chamber between radiative coolers and the surroundings, owing to lack of suitable wind cover materials. Thus, the inverted cone structures can also block the wind from the large zenith angle and reduce the NRHE for the ordinary RC devices.

Recent advances in non-reciprocal transmission have presented great opportunities for RC technology. Non-reciprocal transmission generally needs to break the Lorentz reciprocity, which can be achieved in many ways, that is, magneto-optical media [61−63], non-linear materials [64], photonic crystals [65], chiral structures [66,67], and metamaterials [68,69]. Most of these non-reciprocal transmission structures need additional energy input for spatial time modulation, and the modeling spectral range is narrow. Moreover, the forward-backward transmission ratio of the structures is relatively low, and most structures focus on the shortwave range and microwave range.

However, the composite gratings with a relatively simple structure and no need of additional energy input for modulation [70−72] can be used for RC non-reciprocal transmission. By analogy with visible light and microwave non-reciprocal transmission structures, the mid-infrared non-reciprocal transmission with broadband and high forward-backward transmission ratio can be realized theoretically. The periodic microstructures of inverted trapezoidal cross section made of silver can achieve forward-backward non-reciprocal transmission with a ratio of 2:1 in the wavelength range of 8−13 μm and recover 57% of the cooling power in high humidity areas (Fig. 4c) [73]. If the non-reciprocal transmission within a wider infrared wavelength range can be achieved, the atmospheric radiation absorption can be effectively reduced and the cooling power will be greatly improved.

4.2. Controllable cooling power

All radiative coolers discussed previously are static, whereas in practice, the ambient is always changing. Especially for BC, if radiative coolers always run with the static power, indoor super-cooling may occur at night or in transition season and winter, leading to worse indoor comfort. A feasible solution is to integrate radiative coolers with air conditioning system, which can actively control the access or disconnection of RC modules, at the cost of high energy consumption. Another feasible solution is to use dynamic radiative coolers, which can be realized in many methods, for example, electrically tunable materials (semiconductor quantum wells [74,75], graphene [76]), thermal tunable materials (SiN_x) [77] and phase-changing materials ($Ge_2Sb_2Te_5$ [78,79], VO_2 [80,81], $La_{0.7}Ca_{0.3-x}Sr_xMnO_3$ [82,83]). Electrically tunable materials and thermal tunable materials require not only additional energy input to convert dynamic radiation intensity but also complex structure and high preparation cost. For $Ge_2Sb_2Te_5$, the preparation conditions can be regulated to control the two phases that is, the amorphous and crystalline phases. And the formation of two kinds of mixed phases can also be controlled. However, it is worth noting that the infrared emission profiles of $Ge_2Sb_2Te_5$ with specific morphology do not vary with the temperature [78], thus the material cannot meet the needs of dynamic RC in practice.

VO_2 has a semiconductor-to-metal phase transition at a critical temperature of around 68 °C [84]. Moreover, the phase transition temperature of VO_2 can be adjusted to room temperature by doping W or Mo [85,86] and interfacial strain [87]. However, VO_2 is the negative emittance switching material (i.e. emissivity decreases

with increasing the temperature). High-reflection substrates (e.g. Al) can be introduced to solve the problem by interference. The tunability of VO_2 deposited directly on aluminum plate is only 0.21−0.34 [88]. By introducing insulators such as SiO_2, MgF_2, or TiO_2 into VO_2 and aluminum layers, a destructive interference can be formed to increase the tunability of VO_2 (Fig. 4d and e) [86,89,90]. In addition, it is also viable to increase the infrared absorptivity of VO_2 in high temperature metal state based on the plasma resonance [91]. However, for DRC, this structure will absorb abundant sunlight and cannot achieve effective cooling under the direct sunlight. It is crucial to attach a filter layer, which can not only suppress the solar absorption but also tailor the infrared emission (Fig. 4f) [89].

The aforementioned dynamic RC structures are only suitable to work at night or in transitional season, while for winter, the structures fail to control temperature effectively. Through reasonable design, the VO_2 emitter has low solar absorptivity in high temperature metal state and high solar absorptivity in low temperature semiconductor state. Thus, the VO_2 emitter can not only achieve RC in summer but also provide heating in winter and reduce the negative impact of RC through solar absorption at the same time (Fig. 4f) [90]. Similarly, lanthanum manganese perovskite $La_{0.7}Ca_{0.3-x}Sr_xMnO_3$ also undergoes phase transition with the change of ambient temperature, and the amount of doping can be controlled to adjust the phase transition temperature. Different from VO_2, $La_{0.7}Ca_{0.3-x}Sr_xMnO_3$ has a metal-insulator transition, which means that the material can work directly without additional materials. However, the relatively low emissivity at high temperature affects its actual performance, and further research is essential to improve its emissivity (Fig. 4g) [92].

4.3. Limited sky-facing area

The surface of the radiative coolers is generally facing the sky, which means that the competition of the limited sky-facing area with the mature solar energy systems is inevitable, especially for multistorey or high-rise buildings in cities. There are three feasible solutions: (1) to maximize the net cooling power and reduce the RC areas; (2) to use the side wall for RC technology; and (3) to integrate with solar energy systems (e.g. photovoltaic and photothermic) to make full use of the limited sky-facing area. The development of non-reciprocal transmission may promote radiative coolers to absorb less radiation from the surroundings, that is, radiative coolers can be placed on the larger side wall (although net cooling power could be reduced relative to radiative coolers on the roof)T.

Reducing the RC area cannot fundamentally address the problem, especially for high-rise buildings. And there still require more efforts to investigate the application of non-reciprocal transmission in the mid-infrared wavelength range. Thus, on the premise of less impact on the respective operating efficiency of solar energy systems and RC devices, comprehensive utilization of limited roof area is the effective solution to solve this challenge. The differences of operating time and effective wavelength range in solar energy systems and RC devices provide the basis for integrating these two clean energy technology, that is, the comprehensive utilization of photovoltaic and RC (PV-RC), photothermal and RC (PT-RC), and photovoltaic, photothermal, and RC (PV-PT-RC).

PV-RC is similar to PC, and it is conducive to the improvement of photoelectric conversion efficiency. At the same time, RC can be achieved at night (Fig. 5b) [93,94]. Nevertheless, RC during the day increases the heat dissipation and reduces the efficiency of photothermal devices to a certain extent (Fig. 5a and d) [95,96]. In addition, it is worth noting that the widely used silicon-based photovoltaic devices only use 0.3−1.1 μm wavelength range of sunlight, and the rest near-infrared wavelength range is effective for photothermal devices. Different effective wavelength range provides the basis for the PV-PT-RC system, which can not only improve photovoltaic efficiency but also effectively use solar energy in the daytime and provide cooling at night [97,98]. However, the peak of cooling load appears during the daytime, and it is hard to realize daytime RC with the three aforementioned comprehensive utilization methods.

To achieve both PV/PT and RC during the daytime, the solar absorption materials should have a high transmissivity in the mid-infrared wavelength range. Germanium and silicon can meet this requirement, but reasonable design is essential in practical
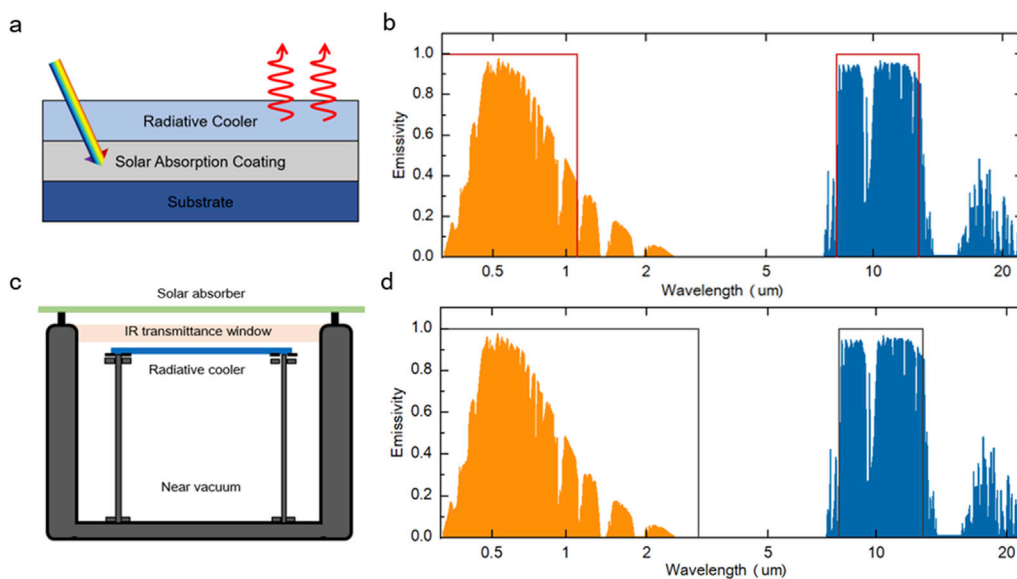

Fig. 5. Comprehensive utilization of limited sky-facing area. (a) Schematic of the PT-RC. (b) The idealized spectral emissivity of the selective PV-RC in the 0.3−22 μm band. (c) Schematic of the experimental setup for the combination of PT/PV and DRC [99]. Reproduced with permission from Chen et al., Joule 3 (2019) 101−110. Copyright 2019 Elsevier. (d) The idealized spectral emissivity of the selective PT-RC in the 0.3−22 μm band. [For both (b) and (d), the AM 1.5 solar spectrum (orange) and typical atmospheric transmittance (blue) are provided for reference]. PT-RC = photothermal and radiative cooling, PV-RC = photovoltaic and radiative cooling, PT/PV = photothermic/photovoltaic.

application (Fig. 5c) [99]. Nevertheless, the comprehensive utilization of solar energy and RC technology is inseparable from the thermal and cold storage device [100,101], and the combination with phase-change materials can effectively promote the commercial application of the integrated systems [102].

5. Outlook

Most RC applications require wind cover to improve the net cooling power, to protect radiative coolers, and to improve the stability of RC devices. However, there exist no desirable materials except thin polyethylene. Therefore, the first step of large-scale application is to develop a suitable wind cover for the subambient RC technology. In addition, radiative coolers mainly consist of the emissive layer and the reflective layer, impeding the application of some emitters. With the development of photonics, the combination of the reflective layer and the emissive layer can be more flexible. For instance, the reflective layer above the emitters can not only suppress the sunlight absorption but also act as a cover shield.

In brief, the net cooling power can be improved and controlled according to the ambient temperature with the development of nanophotonics, non-reciprocal transmission, and phase-change optical materials. In the near future, RC will be comparable with the traditional vapor-compression refrigeration because of its advantages, for example, low cooling cost, energy saving, and no environmental pollution.

Conflict of interests

The authors declare no competing interests.

Acknowledgments

References

[1] T.E. Johnson, Radiation cooling of structures with infrared transparent wind screens, Sol. Energy 17 (1975) 173−178.
[2] C.G. Granqvist, A. Hjortsberg, Surfaces for radiative cooling: silicon monoxide films on aluminum, Appl. Phys. Lett. 36 (1980) 139−141.
[3] C.G. Granqvist, A. Hjortsberg, Radiative cooling to low temperatures: general considerations and application to selectively emitting SiO films, J. Appl. Phys. 52 (1981) 4205−4220.
[4] P. Berdahl, M. Martin, W.P. Beach, Emissivity of clear skies, Sol. Energy 32 (1984) 663−664.
[5] T.M.J. Nilsson, G.A. Niklasson, Radiative cooling during the day: simulations and experiments on pigmented polyethylene cover foils, Sol. Energy Mater. Sol. Cells 37 (1995) 93−118.
[6] A.P. Raman, M.A. Anoma, L. Zhu, E. Rephaeli, S. Fan, Passive radiative cooling below ambient air temperature under direct sunlight, Nature 515 (2014) 540−544.
[7] Y. Zhai, Y. Ma, S.N. David, D. Zhao, R. Lou, G. Tan, R. Yang, X. Yin, Scalable-manufactured randomized glass-polymer hybrid metamaterial for daytime radiative cooling, Science 355 (2017) 1062−1066.
[8] J. Mandal, Y. Fu, A. Overvig, M. Jia, K. Sun, N. Shi, H. Zhou, X. Xiao, N. Yu, Y. Yang, Hierarchically porous polymer coatings for highly efficient passive daytime radiative cooling, Science 362 (2018) 315−319.
[9] M. Li, Y. Jiang, C.F.M. Coimbra, On the determination of atmospheric long-wave irradiance under all-sky conditions, Sol. Energy 144 (2017) 40−48.
[10] F. Kasten, G. Czeplak, Solar and terrestrial radiation dependent on the amount and type of cloud, Sol. Energy 24 (1980) 177−189.
[11] S. Kumar, S.C. Mullick, Wind heat transfer coefficient in solar collectors in outdoor conditions, Sol. Energy 84 (2010) 956−963.
[12] S. Armstrong, W.G. Hurley, A thermal model for photovoltaic panels under varying atmospheric conditions, Appl. Therm. Eng. 30 (2010) 1488−1495.
[13] A.W. Harrison, Radiative cooling of TiO$_2$ white paint, Sol. Energy 20 (1978) 185−188.
[14] S.N. Bathgate, S.G. Bosi, A robust convection cover material for selective radiative cooling applications, Sol. Energy Mater. Sol. Cells 95 (2011) 2778−2785.
[15] X. Ao, M. Hu, B. Zhao, N. Chen, G. Pei, C. Zou, Preliminary experimental study of a specular and a diffuse surface for daytime radiative cooling, Sol. Energy Mater. Sol. Cells 191 (2019) 290−296.
[16] M.A. Kecebas, M.P. Menguc, A. Kosar, K. Sendur, Passive radiative cooling design with broadband optical thin-film filters, J. Quant. Spectrosc. Radiat. Transf. 198 (2017) 1339−1351.
[17] A.R. Gentle, G.B. Smith, A subambient open roof surface under the mid-summer sun, Adv. Sci. 2 (2015) 1500119.
[18] E. Rephaeli, A. Raman, S. Fan, Ultrabroadband photonic structures to achieve high-performance daytime radiative cooling, Nano Lett. 13 (2013) 1457−1461.
[19] Z. Huang, X. Ruan, Nanoparticle embedded double-layer coating for daytime radiative cooling, Int. J. Heat Mass Transf. 104 (2017) 890−896.
[20] H. Bao, C. Yan, B. Wang, X. Fang, C.Y. Zhao, X. Ruan, Double-layer nanoparticle-based coatings for efficient terrestrial radiative cooling, Sol. Energy Mater. Sol. Cells 168 (2017) 78−84.
[21] S. Atiganyanun, J.B. Plumley, S.J. Han, K. Hsu, J. Cytrynbaum, T.L. Peng, S.M. Han, S.E. Han, Effective radiative cooling by paint-format microsphere-based photonic random media, ACS Photonics 5 (2018) 1181−1187.
[22] T. Li, Y. Zhai, S. He, W. Gan, Z. Wei, M. Heidarinejad, D. Dalgo, R. Mi, X. Zhao, J. Song, J. Dai, C. Chen, A. Aili, A. Vellore, A. Martini, R. Yang, J. Srebric, X. Yin, L. Hu, A radiative cooling structural material, Science 364 (2019) 760−763.
[23] N. Li, J. Wang, D. Liu, X. Huang, Z. Xu, C. Zhang, Z. Zhang, M. Zhong, Selective spectral optical properties and structure of aluminum phosphate for daytime passive radiative cooling application, Sol. Energy Mater. Sol. Cells 194 (2019) 103−110.
[24] Z. Chen, L. Zhu, A. Raman, S. Fan, Radiative cooling to deep sub-freezing temperatures through a 24-h day-night cycle, Nat. Commun. 7 (2016) 13729.
[25] B. Bhatia, A. Leroy, Y. Shen, L. Zhao, M. Gianello, D. Li, T. Gu, J. Hu, M. Soljačić, E.N. Wang, Passive directional sub-ambient daytime radiative cooling, Nat. Commun. 9 (2018) 5001.
[26] A. Hervé, J. Drévillon, Y. Ezzahri, K. Joulain, Radiative cooling by tailoring surfaces with microstructures: association of a grating and a multi-layer structure, J. Quant. Spectrosc. Radiat. Transf. 221 (2018) 155−163.
[27] P. Moitra, B.A. Slovick, W. Li, I.I. Kravchencko, D.P. Briggs, S. Krishnamurthy, J. Valentine, Large-scale all-dielectric metamaterial perfect reflectors, ACS Photonics 2 (2015) 692−698.
[28] P. Moitra, B.A. Slovick, Z. Gang Yu, S. Krishnamurthy, J. Valentine, Experimental demonstration of a broadband all-dielectric metamaterial perfect reflector, Appl. Phys. Lett. 104 (2014) 171102.
[29] H.U.Y. Uan, C.H.Y. Ang, X.I.Z. Heng, W.M.U. En, Z. Hen, W. Ang, W.E.Y. Uan, Y.U.Z. Hang, C.H.C. Hen, X.U.L. Iu, Effective, angle-independent radiative cooler based on one-dimensional photonic crystal, Opt. Express 26 (2018) 27885−27893.
[30] D. Wu, C. Liu, Z. Xu, Y. Liu, Z. Yu, L. Yu, L. Chen, R. Li, R. Ma, H. Ye, The design of ultra-broadband selective near-perfect absorber based on photonic structures to achieve near-ideal daytime radiative cooling, Mater. Des. 139 (2018) 104−111.
[31] M.M. Hossain, B. Jia, M. Gu, A metamaterial emitter for highly efficient radiative cooling, Adv. Opt. Mater. 3 (2015) 1047−1051.
[32] C. Zou, G. Ren, M.M. Hossain, S. Nirantar, W. Withayachumnankul, T. Ahmed, M. Bhaskaran, S. Sriram, M. Gu, C. Fumeaux, Metal-loaded dielectric resonator metasurfaces for radiative cooling, Adv. Opt. Mater. 5 (2017) 1700460.
[33] A.R. Gentle, G.B. Smith, Radiative heat pumping from the Earth using surface phonon resonant nanoparticles, Nano Lett. 10 (2010) 373−379.
[34] P. Yang, C. Chen, Z.M. Zhang, A dual-layer structure with record-high solar reflectance for daytime radiative cooling, Sol. Energy 169 (2018) 316−324.
[35] J. Kou, Z. Jurado, Z. Chen, S. Fan, A.J. Minnich, Daytime radiative cooling using near-black infrared emitters, ACS Photonics 4 (2017) 626−630.
[36] Bai Liu, Ni Fang, Xu Lu, A pragmatic bilayer selective emitter for efficient radiative cooling under direct sunlight, Materials 12 (2019) 1208.
[37] Y. Fu, J. Yang, Y.S. Su, W. Du, Y.G. Ma, Daytime passive radiative cooler using porous alumina, Sol. Energy Mater. Sol. Cells 191 (2019) 50−54.
[38] D. Beysens, M. Muselli, I. Milimouk, C. Ohayon, S.M. Berkowicz, E. Soyeux, M. Mileta, P. Ortega, Application of passive radiative cooling for dew condensation, Energy 31 (2006) 2303−2315.
[39] P.N. Nwosu, D. Agbiogwu, Thermal analysis of a novel fibre-reinforced plastic solar hot water storage tank, Energy 60 (2013) 109−115.
[40] E.A. Goldstein, A.P. Raman, S. Fan, Sub-ambient non-evaporative fluid cooling with the sky, Nat. Energy 2 (2017) 17143.
[41] D. Zhao, A. Aili, Y. Zhai, J. Lu, D. Kidd, G. Tan, X. Yin, R. Yang, Subambient cooling of water: toward real-world applications of daytime radiative cooling, Joule 3 (2019) 111−123.
[42] W. Shockley, H.J. Queisser, Detailed balance limit of efficiency of p-n junction solar cells, J. Appl. Phys. 32 (1961) 510.
[43] E. Skoplaki, J.A. Palyvos, On the temperature dependence of photovoltaic module electrical performance: a review of efficiency/power correlations, Sol. Energy 83 (2009) 614−624.
[44] L. Zhu, A. Raman, K.X. Wang, M.A. Anoma, S. Fan, Radiative cooling of solar cells, Optica 1 (2014) 32.
[45] L. Zhu, A.P. Raman, S. Fan, Radiative cooling of solar absorbers using a visibly transparent photonic crystal thermal blackbody, Proc. Natl. Acad. Sci. 112 (2015) 12282−12287.
[46] A.R. Gentle, G.B. Smith, Is enhanced radiative cooling of solar cell modules worth pursuing? Sol. Energy Mater. Sol. Cells 150 (2016) 39−42.

[47] Y. Lu, Z. Chen, L. Ai, X. Zhang, J. Zhang, J. Li, W. Wang, R. Tan, N. Dai, W. Song, A universal route to realize radiative cooling and light management in photovoltaic modules, Sol. RRL 1 (2017) 1700084.

[48] W. Li, Y. Shi, K. Chen, L. Zhu, S. Fan, A comprehensive photonic approach for solar cell cooling, ACS Photonics 4 (2017) 774–782.

[49] B. Zhao, M. Hu, X. Ao, Q. Xuan, G. Pei, Comprehensive photonic approach for diurnal photovoltaic and nocturnal radiative cooling, Sol. Energy Mater. Sol. Cells 178 (2018) 266–272.

[50] K. Nishioka, Y. Ota, K. Tamura, K. Araki, Heat reduction of concentrator photovoltaic module using high radiation coating, Surf. Coat. Technol. 215 (2013) 472–475.

[51] Z.G. Zhou, X.S. Sun, P. Bermel, Radiative cooling for thermophotovoltaic systems, Infrared Rem. Sens. Instrum. 9973 (2016). UNSP 997308.

[52] S.J. Byrnes, R. Blanchard, F. Capasso, Harvesting renewable energy from Earth's mid-infrared emissions, Proc. Natl. Acad. Sci. 111 (2014) 3927–3932.

[53] F. Pauly, J.C. Cuevas, D. Natelson, D.R. Ward, F. Hu, Optical rectification and field enhancement in a plasmonic nanogap, Nat. Nanotechnol. 5 (2010) 732–736.

[54] M.W. Knight, H. Sobhani, P. Nordlander, N.J. Halas, Photodetection with active optical antennas, Science 332 (2011) 702–704.

[55] R.G. Bedford, G. Triplett, D.H. Tomich, S.W. Koch, J. Moloney, J. Hader, Reduced auger recombination in mid-infrared semiconductor lasers, J. Appl. Phys. 110 (2011), 073108.

[56] Z. Yu, N.P. Sergeant, G. Zhang, H. Wang, S. Fan, Enhancing far-field thermal emission with thermal extraction, Nat. Commun. 4 (2013) 1730.

[57] J. Shi, B. Liu, P. Li, L.Y. Ng, S. Shen, Near-field energy extraction with hyperbolic metamaterials, Nano Lett. 15 (2015) 1217–1221.

[58] J. Liu, D. Zhang, S. Jiao, J. Ling, J. Zhang, Z. Zhou, Z. Zhang, Radiative Cooling with Nanoporous Polyethylene Film, in press.

[59] C.Y. Tso, K.C. Chan, C.Y.H. Chao, A field investigation of passive radiative cooling under Hong Kong's climate, Renew. Energy 106 (2017) 52–61.

[60] A.F.G. Jacobs, B.G. Heusinkveld, S.M. Berkowicz, Passive dew collection in a grassland area, The Netherlands, Atmos. Res. 87 (2008) 377–385.

[61] L.D. Tzuang, K. Fang, P. Nussenzveig, S. Fan, M. Lipson, Non-reciprocal phase shift induced by an effective magnetic flux for light, Nat. Photonics 8 (2014) 701–705.

[62] N.A. Estep, D.L. Sounas, J. Soric, A. Alù, Magnetic-free non-reciprocity and isolation based on parametrically modulated coupled-resonator loops, Nat. Phys. 10 (2014) 923–927.

[63] F. Ruesink, M.A. Miri, A. Alù, E. Verhagen, Nonreciprocity and magnetic-free isolation based on optomechanical interactions, Nat. Commun. 7 (2016) 13662.

[64] L. Fan, J. Wang, L.T. Varghese, H. Shen, B. Niu, Y. Xuan, A.M. Weiner, M. Qi, An all-silicon passive optical diode, Science 335 (2012) 447–450.

[65] C. Wang, X.L. Zhong, Z.Y. Li, Linear and passive silicon optical isolator, Sci. Rep. 2 (2012) 674.

[66] A.S. Schwanecke, A. Krasavin, D.M. Bagnall, A. Potts, A.V. Zayats, N.I. Zheludev, Broken time reversal of light interaction with planar chiral nanostructures, Phys. Rev. Lett. 91 (2003) 1–4.

[67] L. Stephen, N. Yogesh, V. Subramanian, Broadband asymmetric transmission of linearly polarized electromagnetic waves based on chiral metamaterial, J. Appl. Phys. 123 (2018), 033103.

[68] T. Xu, H.J. Lezec, Visible-frequency asymmetric transmission devices incorporating a hyperbolic metamaterial, Nat. Commun. 5 (2014) 1–7.

[69] G. Kenanakis, A. Xomalis, A. Selimis, M. Vamvakaki, M. Farsari, M. Kafesaki, C.M. Soukoulis, E.N. Economou, Three-dimensional infrared metamaterial with asymmetric transmission, ACS Photonics 2 (2015) 287–294.

[70] B. Tang, Z. Li, Z. Liu, F. Callewaert, K. Aydin, Broadband asymmetric light transmission through tapered metallic gratings at visible frequencies, Sci. Rep. 6 (2016) 39166.

[71] M. Stolarek, D. Yavorskiy, R. Kotyński, C.J. Zapata Rodríguez, J. Łusakowski, T. Szoplik, Asymmetric transmission of terahertz radiation through a double grating, Opt. Lett. 38 (2013) 839.

[72] S. Cakmakyapan, A.E. Serebryannikov, H. Caglayan, E. Ozbay, Spoof-plasmon relevant one-way collimation and multiplexing at beaming from a slit in metallic grating, Opt. Express 20 (2012) 26636.

[73] R.Y.M. Wong, C.Y. Tso, C.Y.H. Chao, B. Huang, M.P. Wan, Ultra-broadband asymmetric transmission metallic gratings for subtropical passive daytime radiative cooling, Sol. Energy Mater. Sol. Cells 186 (2018) 330–339.

[74] T. Inoue, M. De Zoysa, T. Asano, S. Noda, Realization of dynamic thermal emission control, Nat. Mater. 13 (2014) 928–931.

[75] M. De Zoysa, T. Asano, K. Mochizuki, A. Oskooi, T. Inoue, Conversion of broadband to narrowband thermal emission through energy recycling, Nat. Photonics 6 (2012) 535–539.

[76] V.W. Brar, M.C. Sherrott, M.S. Jang, S. Kim, L. Kim, M. Choi, L.A. Sweatlock, H.A. Atwater, Electronic modulation of infrared radiation in graphene plasmonic resonators, Nat. Commun. 6 (2015) 7032.

[77] X. Liu, W.J. Padilla, Thermochromic infrared metamaterials, Adv. Mater. 28 (2016) 871–875.

[78] K. Du, Q. Li, Y. Lyu, J. Ding, Y. Lu, Z. Cheng, M. Qiu, Control over emissivity of zero-static-power thermal emitters based on phase changing material GST, Light Sci. Appl. 6 (2017): e16194.

[79] Z.J. Coppens, J.G. Valentine, Spatial and temporal modulation of thermal emission, Adv. Mater. 29 (2017) 1701275.

[80] M.M. Qazilbash, M. Brehm, B.-G. Chae, P.-C. Ho, G.O. Andreev, B.-J. Kim, S.J. Yun, A.V. Balatsky, M.B. Maple, F. Keilmann, H.-T. Kim, D.N. Basov, Mott transition in VO2 revealed by infrared spectroscopy and nano-imaging, Science 318 (2007) 1750–1753.

[81] S. Lee, K. Hippalgaonkar, F. Yang, J. Hong, C. Ko, J. Suh, K. Liu, K. Wang, J.J. Urban, X. Zhang, C. Dames, S.A. Hartnoll, O. Delaire, J. Wu, Anomalously low electronic thermal conductivity in metallic vanadium dioxide, Science 355 (2017) 371–374.

[82] F. Jin, H. Zhang, Q. Chen, Improved curie temperature and temperature co-efficient of resistance (TCR) in La0.7Ca0.3-xSrxMnO3:Ag0.2 composites, J. Alloy. Comp. 747 (2018) 1027–1032.

[83] T. Sun, J. Jiang, Q. Chen, X. Liu, Improvement of room-temperature TCR and MR in polycrystalline La0.67(Ca0.27Sr0.06) MnO3 ceramics by Ag2O doping, Ceram. Int. 44 (2018) 9865–9874.

[84] F. Induced, J. Jeong, N. Aetukuri, T. Graf, T.D. Schladt, M.G. Samant, S.S.P. Parkin, Suppression of metal-insulator transition, Science 339 (2013) 1402–1406.

[85] A. Hendaoui, N. Émond, S. Dorval, M. Chaker, E. Haddad, Enhancement of the positive emittance-switching performance of thermochromic VO2 films deposited on Al substrate for an efficient passive thermal control of space-crafts, Curr. Appl. Phys. 13 (2013) 875–879.

[86] A. Hendaoui, N. Émond, S. Dorval, M. Chaker, E. Haddad, VO2-based smart coatings with improved emittance-switching properties for an energy-efficient near room-temperature thermal control of spacecrafts, Sol. Energy Mater. Sol. Cells 117 (2013) 494–498.

[87] L.L. Fan, S. Chen, Z.L. Luo, Q.H. Liu, Y.F. Wu, L. Song, D.X. Ji, P. Wang, W.S. Chu, C. Gao, C.W. Zou, Z.Y. Wu, Strain dynamics of ultrathin VO2 film grown on TiO2(001) and the associated phase transition modulation, Nano Lett. 14 (2014) 4036–4043.

[88] M. Benkahoul, M. Chaker, J. Margot, E. Haddad, R. Kruzelecky, B. Wong, W. Jamroz, P. Poinas, Thermochromic VO2 film deposited on Al with tunable thermal emissivity for space applications, Sol. Energy Mater. Sol. Cells 95 (2011) 3504–3508.

[89] M. Ono, K. Chen, W. Li, S. Fan, Self-adaptive radiative cooling based on phase change materials, Opt. Express 26 (2018) A777–A787.

[90] W.J.M. Kort-kamp, S. Kramadhati, A.K. Azad, M.T. Reiten, D.A.R. Dalvit, Passive radiative " thermostat " enabled by phase-change photonic nano-structures, ACS Photonics 5 (2018) 4554–4560.

[91] K. Sun, C.A. Riedel, A. Urbani, M. Simeoni, M. Zalkovskij, B. Bilenberg, C.H. De Groot, O.L. Muskens, VO2 thermochromic metamaterial-based smart optical solar reflector, ACS Photonics 5 (2018) 2280–2286.

[92] D. Fan, Q. Li, Y. Xuan, H. Tan, J. Fang, Temperature-dependent infrared properties of Ca doped (La,Sr)MnO3 compositions with potential thermal control application, Appl. Therm. Eng. 51 (2013) 255–261.

[93] B. Zhao, M. Hu, X. Ao, G. Pei, Conceptual development of a building-integrated photovoltaic–radiative cooling system and preliminary performance analysis in Eastern China, Appl. Energy 205 (2017) 626–634.

[94] M. Hu, B. Zhao, X. Ao, J. Feng, J. Cao, Y. Su, G. Pei, Experimental study on a hybrid photo-thermal and radiative cooling collector using black acrylic paint as the panel coating, Renew. Energy 139 (2019) 1217–1226.

[95] M. Hu, G. Pei, Q. Wang, J. Li, Y. Wang, J. Ji, Field test and preliminary analysis of a combined diurnal solar heating and nocturnal radiative cooling system, Appl. Energy 179 (2016) 899–908.

[96] M. Hu, B. Zhao, X. Ao, Y. Su, Y. Wang, G. Pei, Comparative analysis of different surfaces for integrated solar heating and radiative cooling: a numerical study, Energy 155 (2018) 360–369.

[97] M. Hu, B. Zhao, X. Ao, P. Zhao, Y. Su, G. Pei, Field investigation of a hybrid photovoltaic-photothermic-radiative cooling system, Appl. Energy 231 (2018) 288–300.

[98] M. Hu, B. Zhao, J. Li, Y. Wang, G. Pei, Preliminary thermal analysis of a combined photovoltaic–photothermic–nocturnal radiative cooling system, Energy 137 (2017) 419–430.

[99] Z. Chen, L. Zhu, W. Li, S. Fan, Simultaneously and synergistically harvest energy from the sun and outer space, Joule 3 (2019) 101–110.

[100] D. Zhao, C.E. Martini, S. Jiang, Y. Ma, Y. Zhai, G. Tan, X. Yin, R. Yang, Development of a single-phase thermosiphon for cold collection and storage of radiative cooling, Appl. Energy 205 (2017) 1260–1269.

[101] Z. Zhou, J. Liu, C. Wang, X. Huang, F. Gao, S. Zhang, B. Yu, Research on the application of phase-change heat storage in centralized solar hot water system, J. Clean. Prod. 198 (2018) 1262–1275.

[102] Z. Zhou, Z. Zhang, J. Zuo, K. Huang, L. Zhang, Phase change materials for solar thermal energy storage in residential buildings in cold climate, Renew. Sustain. Energy Rev. 48 (2015) 692–703.

[103] K. Sun, C.A. Riedel, Y. Wang, A. Urbani, M. Simeoni, S. Mengali, M. Zalkovskij, B. Bilenberg, C.H. De Groot, O.L. Muskens, Metasurface optical solar reflectors using AZO transparent conducting oxides for radiative cooling of spacecraft, ACS Photonics 5 (2018) 495–501.